



HAL
open science

The Kv1-associated molecules TAG-1 and Caspr2 are selectively targeted to the axon initial segment in hippocampal neurons

Delphine Pinatel, Bruno Hivert, Margaux Saint-Martin, Nelly Noraz, Maria Savvaki, Domna Karagogeos, Catherine Faivre-Sarrailh

► To cite this version:

Delphine Pinatel, Bruno Hivert, Margaux Saint-Martin, Nelly Noraz, Maria Savvaki, et al.. The Kv1-associated molecules TAG-1 and Caspr2 are selectively targeted to the axon initial segment in hippocampal neurons. *Journal of Cell Science*, 2017, 130 (13), pp.2209-2220. 10.1242/jcs.202267 . hal-02347254

HAL Id: hal-02347254

<https://hal.science/hal-02347254>

Submitted on 5 Nov 2019

HAL is a multi-disciplinary open access archive for the deposit and dissemination of scientific research documents, whether they are published or not. The documents may come from teaching and research institutions in France or abroad, or from public or private research centers.

L'archive ouverte pluridisciplinaire **HAL**, est destinée au dépôt et à la diffusion de documents scientifiques de niveau recherche, publiés ou non, émanant des établissements d'enseignement et de recherche français ou étrangers, des laboratoires publics ou privés.

RESEARCH ARTICLE

The Kv1-associated molecules TAG-1 and Caspr2 are selectively targeted to the axon initial segment in hippocampal neurons

Delphine Pinatel¹, Bruno Hivert¹, Margaux Saint-Martin², Nelly Noraz², Maria Savvaki³, Domna Karagogeos³ and Catherine Faivre-Sarrailh^{1,*}

ABSTRACT

Caspr2 and TAG-1 (also known as CNTNAP2 and CNTN2, respectively) are cell adhesion molecules (CAMs) associated with the voltage-gated potassium channels Kv1.1 and Kv1.2 (also known as KCNA1 and KCNA2, respectively) at regions controlling axonal excitability, namely, the axon initial segment (AIS) and juxtaparanodes of myelinated axons. The distribution of Kv1 at juxtaparanodes requires axo-glia contacts mediated by Caspr2 and TAG-1. In the present study, we found that TAG-1 strongly colocalizes with Kv1.2 at the AIS of cultured hippocampal neurons, whereas Caspr2 is uniformly expressed along the axolemma. Live-cell imaging revealed that Caspr2 and TAG-1 are sorted together in axonal transport vesicles. Therefore, their differential distribution may result from diffusion and trapping mechanisms induced by selective partnerships. By using deletion constructs, we identified two molecular determinants of Caspr2 that regulate its axonal positioning. First, the LNG2-EGF1 modules in the ectodomain of Caspr2, which are involved in its axonal distribution. Deletion of these modules promotes AIS localization and association with TAG-1. Second, the cytoplasmic PDZ-binding site of Caspr2, which could elicit AIS enrichment and recruitment of the membrane-associated guanylate kinase (MAGuK) protein MPP2. Hence, the selective distribution of Caspr2 and TAG-1 may be regulated, allowing them to modulate the strategic function of the Kv1 complex along axons.

KEY WORDS: Polarity, Axonal transport, Cell adhesion molecule, Axon initial segment, Juxtaparanode

INTRODUCTION

The axon initial segment (AIS) is a specialized region of neurons where action potentials are initiated. The high density of specific voltage-gated Na⁺ and K⁺ channels gives the AIS unique electrical properties. The voltage-gated Na⁺ channels Nav1.2 and Nav1.6 (also known as SCN2A and SCN8A, respectively) are anchored at the AIS via the ankyrinG scaffold, which is the major organizer of this axonal subdomain (Yoshimura and Rasband, 2014; Zhou et al., 1998). A variety of voltage-gated K⁺ channels are localized at AIS,

including Kv7.2 and Kv7.3 (also known as KCNQ2 and KCNQ3, respectively), Kv1.1 and Kv1.2 (KCNA1 and KCNA2, respectively) and Kv2.1 (KCNB1), which function as modulators of action potential initiation and frequency (Devaux et al., 2004; King et al., 2014; Trimmer, 2015; Van Wart et al., 2007). The Kv7.2 and Kv7.3 channels are tethered at the AIS through ankyrinG binding (Pan et al., 2006), while the mechanisms responsible for Kv2.1 and Kv1.1/Kv1.2 enrichment are poorly understood. The distribution of Kv channels at the AIS and along axon may influence intrinsic excitability and transmitter release (Kole and Stuart, 2012; Rama et al., 2015).

The Kv1 channels co-purify with several cell adhesion molecules (CAMs) including Caspr2 (also known as CNTNAP2), TAG-1 (also known as CNTN2), LGI1 and ADAM22 proteins. These CAMs are autoimmune targets in limbic encephalitis that is associated with voltage-gated K⁺ channels (Irani et al., 2010; Lancaster et al., 2011). The role of Caspr2 and TAG-1 has been well established at the juxtaparanodes of myelinated axons where they mediate axo-glia contacts and induce the clustering of Kv1.1 and Kv1.2 to control the internodal resting potential (Poliak et al., 2003; Traka et al., 2003). The intracellular protein 4.1B (also known as EPB41L3), which binds Caspr2 is required for assembling the juxtaparanodal scaffold (Buttermore et al., 2011; Cifuentes-Diaz et al., 2011; Einheber et al., 2013; Horresh et al., 2010). In contrast to juxtaparanodes, Caspr2, and TAG-1, although present at the AIS are dispensable for the recruitment of Kv1 channels there (Duflocq et al., 2011; Inda et al., 2006; Ogawa et al., 2008). In addition, protein 4.1B is not enriched at the AIS while the membrane-associated guanylate kinase (MAGuK) PSD-93 (also known as DLG2) is present at that site (Duflocq et al., 2011; Ogawa et al., 2008). Other membrane proteins interacting with Kv1 channels could be localized at the AIS. In particular, ADAM22 is recruited at the AIS of cultured hippocampal neurons with PSD-93, but is not required for the clustering of Kv1 channels (Ogawa et al., 2010).

Whether CAMs can modulate Kv1 channel surface expression and activity tuning at the AIS is still unclear. In this regard, it would be important to analyze the molecular mechanisms that are implicated in the recruitment of Caspr2 and TAG-1 at the AIS. We have previously shown that Caspr2 is delivered both to the somatodendritic and axonal compartments in hippocampal neurons, and its polarized expression is achieved through selective endocytosis from the somatodendritic plasma membrane. The cell surface expression of Caspr2 is regulated through an endocytosis motif that overlaps with the 4.1B-binding sequence (Bel et al., 2009). Caspr2 does not interact with type I PDZ proteins, like PSD-93, but may associate with MAGuK proteins of the MPP2 family and MUPP1 (also known as MPDZ) (Horresh et al., 2008; Tanabe et al., 2015). In the present study, we used deletion or chimeric constructs to identify cytoplasmic and extracellular determinants implicated in the AIS versus axonal distribution of Caspr2.

¹Aix-Marseille Université, CNRS, Centre de Recherche en Neurobiologie et Neurophysiologie de Marseille, Marseille UMR7286, France. ²Institut Neuromyogène, CNRS UMR 5310, INSERM U1217, Université Claude Bernard Lyon 1, 69 372 Lyon, France. ³Department of Basic Sciences, University of Crete Medical School and Institute of Molecular Biology and Biotechnology, Foundation for Research and Technology, University of Crete, Heraklion, Crete 711 10, Greece.

*Author for correspondence (catherine.sarrailh@univ-amu.fr)

 D.P., 0000-0001-5514-0551; B.H., 0000-0002-3371-6123; M.S., 0000-0003-2240-4543; N.N., 0000-0003-4076-9773; M.S., 0000-0001-9094-1055; D.K., 0000-0002-8129-9731; C.F., 0000-0002-1718-0533; C.F., 0000-0002-1718-0533

In addition, we examined the interdependence of the two CAMs, Caspr2 and TAG-1 for their axonal transport and targeting.

RESULTS

TAG-1 is enriched at the AIS whereas Caspr2 is expressed along the axon in cultured hippocampal neurons

Caspr2 and TAG-1 have been reported to colocalize with Kv1 channels at the AIS in several neuronal subtypes, such as motor and cortical neurons (Duflocq et al., 2011; Inda et al., 2006). We analyzed the surface expression of endogenous Caspr2 and TAG-1 in hippocampal neurons in culture using live double-immunostaining at 14 days *in vitro* (DIV14). We observed that Caspr2 and TAG-1 were differentially distributed. As previously reported (Pinatel et al., 2015), we used anti-Caspr2 auto-antibodies from patients with limbic encephalitis to show that Caspr2 surface labeling was polarized to axons (Fig. 1A, red), but not

enriched at the AIS, which can be labeled for ankyrinG (Fig. 1A, blue). In contrast, TAG-1 was enriched at the AIS, as shown using mouse anti-TAG-1 monoclonal antibody (mAb) 1C12 (Fig. 1A, green). As observed for endogenous molecules, transfected Caspr2-HA was distributed all along the axonal membrane (Fig. 1B, red), whereas TAG-1-GFP was enriched at the AIS (Fig. 1B, green).

We asked whether the AIS versus axonal distribution of TAG-1-GFP and Caspr2-HA might be correlated with the concentration of Kv1 channels at the AIS. Hippocampal neurons were double-transfected with both CAMs at DIV14, and their surface expression was measured at the AIS and along the axon (Fig. 1C–F). TAG-1-GFP, but not Caspr2-HA, was enriched at the AIS, as also observed for Kv1.2 (Fig. 1C). Quantitative analysis was performed by measuring the ratio of the mean fluorescence intensity at the AIS versus at the axon. The mean AIS:axon ratios were 2.31 ± 0.16 for

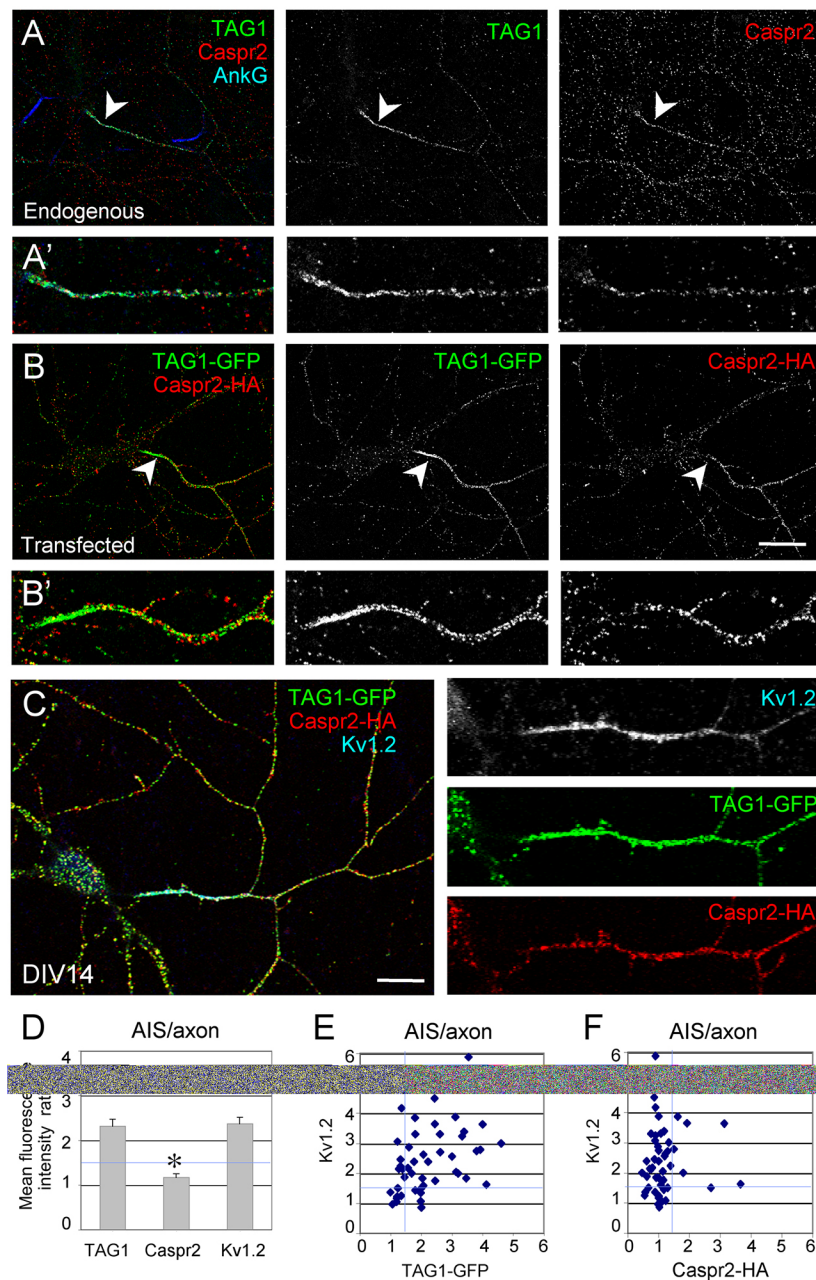


Fig. 1. TAG-1 is enriched at the AIS and Caspr2 is uniformly targeted along the axon in cultured hippocampal neurons. (A,A') Hippocampal neurons at DIV14 were surface labeled using human anti-Caspr2 autoantibodies (red) and mouse anti-TAG-1 1C12 mAb (green), and were then fixed and permeabilized before staining for the AIS marker ankyrinG (blue). Endogenous TAG-1 was enriched at the AIS whereas Caspr2 was uniformly detected along the axon. (B,B') Hippocampal neurons at DIV14 were co-transfected with TAG-1-GFP and Caspr2-HA and surface labeled for GFP (green) and HA (red). The AIS is indicated with arrowheads. (C–F) DIV14 hippocampal neurons were co-transfected with TAG-1-GFP and Caspr2-HA and surface labeled for GFP (green) and HA (red). Neurons were fixed, permeabilized and immunostained for Kv1.2 (blue). The AIS:axon ratio (denoted AIS/axon) of fluorescence intensity was calculated and expressed as the mean \pm s.e.m. ($n=46$) (D), or plotted for individual neurons (E,F). * $P < 0.01$ by comparison with TAG-1 (ANOVA). Note that TAG-1-GFP enrichment at the AIS correlates with the level of AIS enrichment of endogenous Kv1.2, whereas that for Caspr2-HA does not. Scale bars: 20 μ m (B); 10 μ m (C).

TAG-1–GFP, 1.16 ± 0.09 for Caspr2–HA and 2.37 ± 0.15 for Kv1.2 (mean \pm s.e.m.; Fig. 1D). The individual values ($n=46$) were plotted, showing that the AIS:axon ratio for TAG-1 was correlated with the AIS:axon ratio value for the Kv1.2 channel (Fig. 1E). In contrast, Caspr2–HA was not enriched at the AIS of neurons, even in axons where the Kv1.2 channels were highly enriched in the AIS (Fig. 1F). This result indicates that TAG-1 and Kv1 may be anchored to the AIS in a complex within the same scaffold.

Since TAG-1 is a glycosphosphatidylinositol (GPI)-anchored CAM, it does not directly interact with intracellular AIS components. The Ig domains of TAG-1 interact with multiple binding partners including NrCAM and the neurofascin isoform 186 (neurofascin-186) (Fig. S1). These two related CAMs are trapped at the AIS via their ankyrin-binding motif (Davis et al., 1996). Therefore, we analyzed the role of the Ig and fibronectin type III (FnIII) domains of TAG-1 in its enrichment at the AIS (Fig. 2). GFP-tagged full-length TAG-1, and GFP-tagged deletion mutants

TAG-1-Ig (containing only the Ig domain) and TAG-1-Fn (containing only the FnIII domains) (schematized in Fig. 2D) were transfected in hippocampal neurons at DIV14 (Fig. 2A–C). The AIS:axon ratio was significantly reduced for the TAG-1-Ig and TAG-1-Fn deletion mutants (1.38 ± 0.08 and 1.14 ± 0.09 , respectively) compared to that seen for full-length TAG-1 (2.53 ± 0.14) (Fig. 2E). Next, we analyzed the Kv1.2 expression in neurons transfected with TAG-1-Ig and TAG-1-Fn. Kv1.2 (red) was enriched at the AIS labeled for ankyrinG (blue), whereas both TAG-1 deletion mutants (green) were evenly distributed along the axon (Fig. 2G,H). The AIS:axon ratio for Kv1.2 was 2.23 ± 0.15 ($n=26$) and 2.81 ± 0.24 ($n=15$) in neurons transfected with TAG-1-Ig and TAG-1-Fn, respectively. Plotting of individual values did not indicate any correlation between the AIS:axon ratios of Kv1.2 and TAG1 deletion mutants (Fig. 2I,J). Thus, the conformation of the full-length TAG-1 molecule seems to be required for its proper targeting at the AIS. These data also suggest that TAG-1 might be

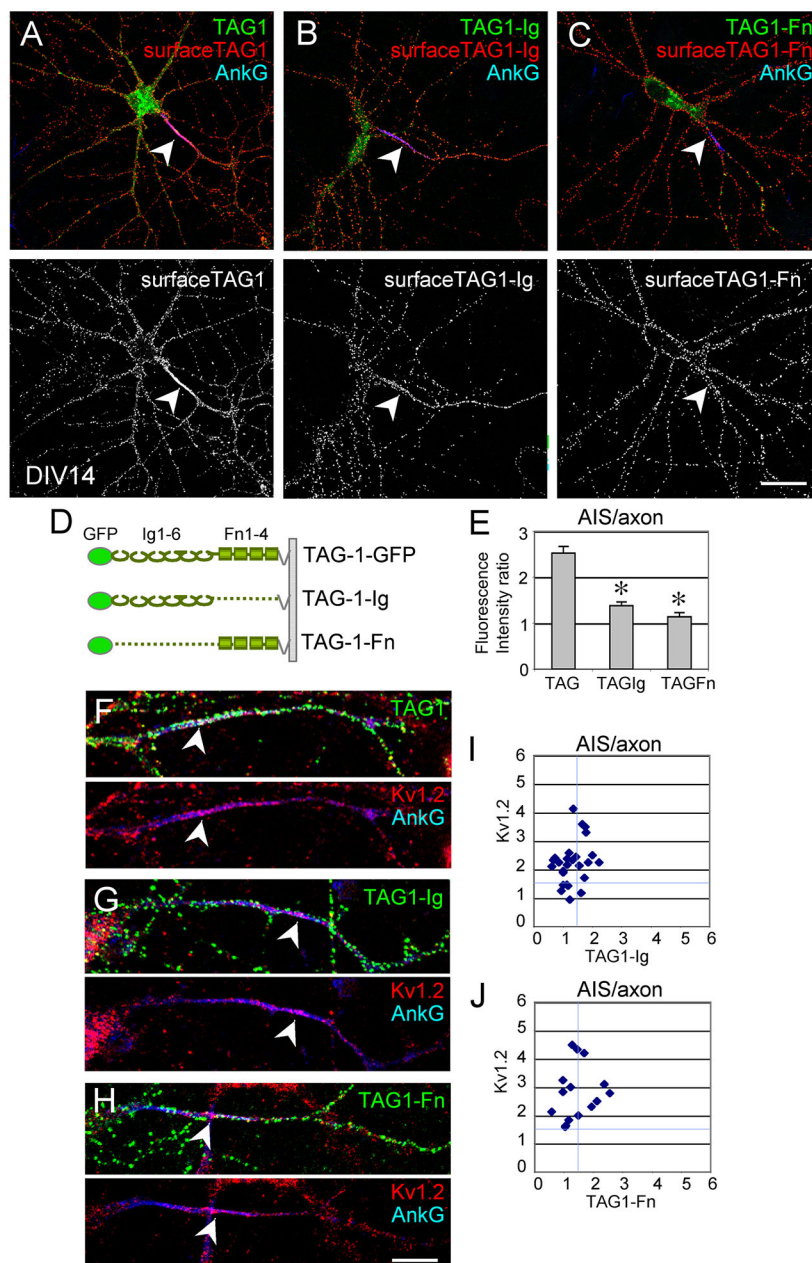


Fig. 2. Deletion of the Ig or FnIII domains of TAG-1 prevents its enrichment at the AIS in cultured hippocampal neurons.

Neurons at DIV14 were transfected with TAG-1–GFP (A,F), TAG-1-Ig (B,G) or TAG-1-Fn (C,H). (A–C) Neurons were surface labeled for GFP (red), then permeabilized and immunostained for ankyrinG (blue). Note that only full-length TAG-1–GFP is highly recruited to the AIS. (D) Schematic drawing of the TAG-1 deletion mutants. (E) AIS:axon ratios of fluorescence intensity (mean \pm s.e.m., $n=18$). * $P < 0.01$ by comparison with full-length TAG-1–GFP (ANOVA). (F–H) Neurons were surface labeled for GFP (green), then permeabilized and immunostained for ankyrinG (blue) and Kv1.2 (red). Arrowheads in A–C and F–H indicate the AIS. (I,J) The AIS:axon ratio (AIS/axon) of fluorescence intensity for TAG-1-Ig or TAG-1-Fn versus Kv1.2 was plotted for individual neurons. Scale bars: 20 μ m (C); 5 μ m (H).

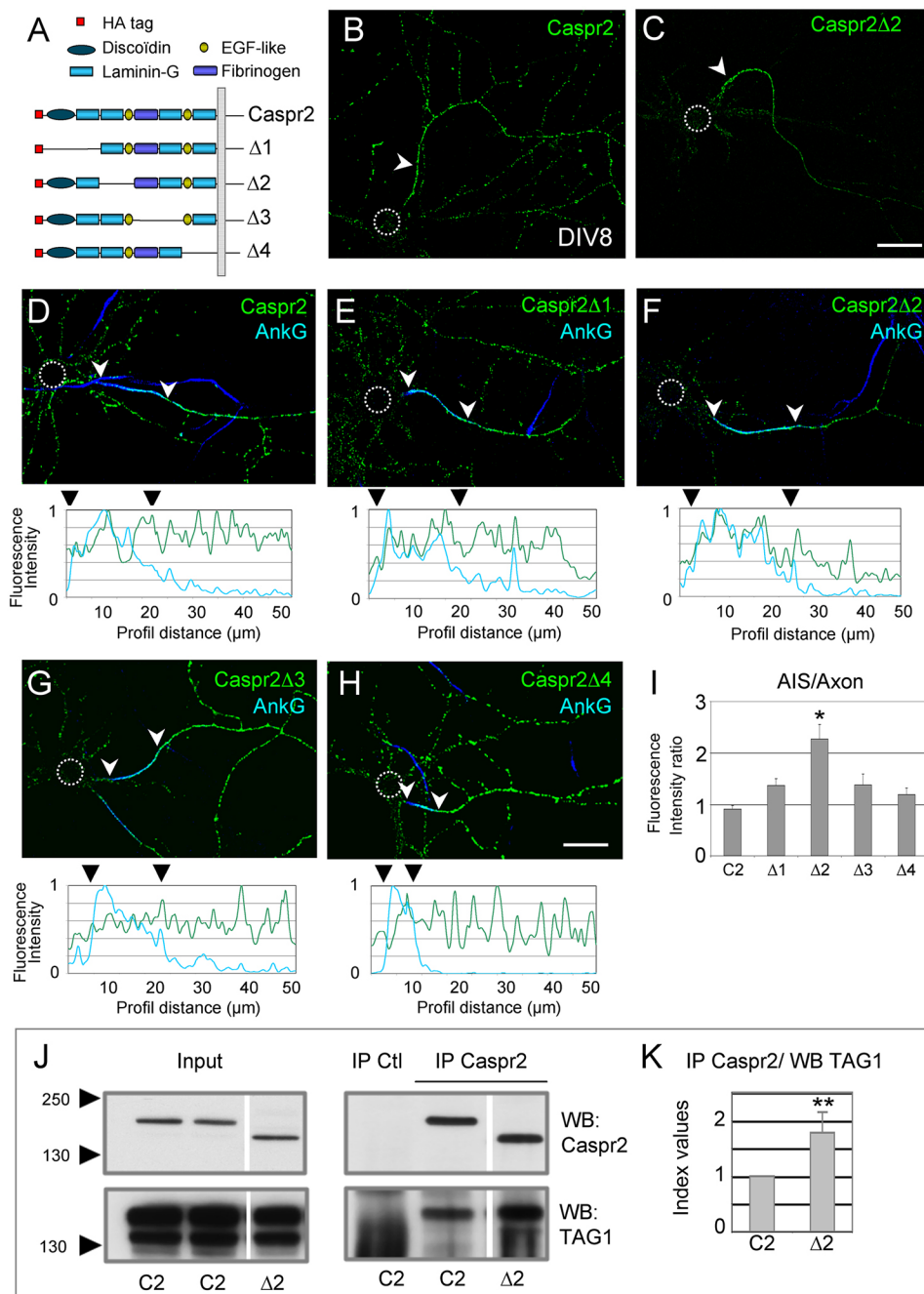
recruited to the Kv1 complex independently of the neurofascin–NrCAM–ankyrinG complex.

The LNG2 and EGF1 modules in the ectodomain of Caspr2 determine its axonal distribution

Next, we addressed the role of the Caspr2 ectodomain in its polarized expression to the axonal surface. We analyzed the distribution of a series of HA-tagged Caspr2 constructs with sequential deletions of modules in the ectodomain (Fig. 3A; Pinatel et al., 2015). After transfection at DIV7, hippocampal neurons were surface labeled for HA (green), and then fixed and permeabilized before staining for ankyrinG as an AIS marker (blue). Strikingly, Caspr2 Δ 2, which has a deletion of the laminin-G2 (LNG2) and EGF-like1 (EGF1) modules, was strongly enriched at the AIS (Fig. 3C,F) by contrast with full-length Caspr2 (Fig. 3B,D). All the

other deletion mutants (Caspr2 Δ 1, Caspr2 Δ 3 and Caspr2 Δ 4) were distributed along the axon (Fig. 3E,G,H). Quantitative analysis indicated that the mean AIS:axon ratio of Caspr2 Δ 2 (2.4 ± 0.4) was significantly increased in comparison with that for full-length Caspr2 (0.95 ± 0.1) (Fig. 3I). We observed that Caspr2 Δ 2 enrichment at the AIS of transfected neurons correlated with the level of endogenous Kv1.2 enrichment by plotting individual values for the AIS:axon ratios ($n=27$) (Fig. S2A–C). Therefore, the LNG2 and EGF1 modules in the ectodomain may exert a dominant effect, promoting the distribution of Caspr2 all along the axon. Alternatively, deletion of these modules may induce a conformational change and influence the association between Caspr2 and TAG-1.

To analyze the interaction between Caspr2 and TAG-1, co-immunoprecipitation experiments were performed using extracts



from HEK cells co-transfected with TAG-1–GFP and Caspr2–HA constructs. As shown in Fig. 3J, both Caspr2 and Caspr2 Δ 2 constructs interacted with TAG-1. Quantitative analysis indicated that the Δ 2 deletion significantly increased co-immunoprecipitation of TAG-1 (+78%, $n=5$) by comparison with full-length Caspr2 (Fig. 3K). Thus, Caspr2 Δ 2 might be enriched at the AIS because of its tight binding with endogenous TAG-1. Deletion of the LNG2 and EGF1 domains in the Caspr2 Δ 2 mutant may induce a conformational change favoring TAG-1 binding or association of the Caspr2 Δ 2 cytoplasmic tail to scaffolding molecules.

Caspr2 and TAG-1 are colocalized in axonal transport vesicles

Caspr2 and TAG-1 are known to interact in cis (Fig. 3J; Traka et al., 2003). However, they are differentially distributed along the axon, as TAG-1 is enriched at the AIS whereas Caspr2 evenly detected all along the axon. We performed time-lapse recording of neurons transfected at DIV7 with Caspr2–mCherry and TAG-1–GFP to get some insight into their axonal-targeting mechanisms (Fig. 4). The

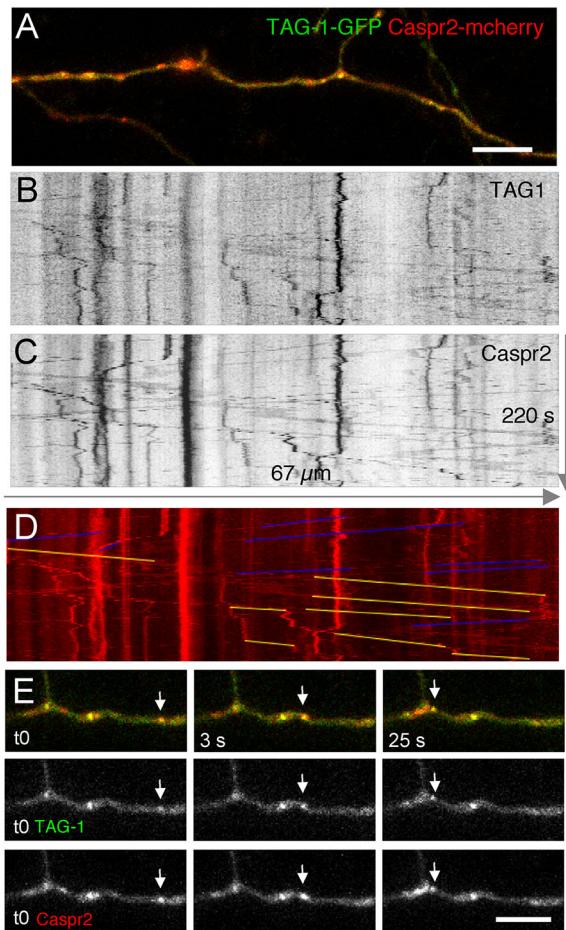


Fig. 4. Caspr2 and TAG-1 are colocalized within axonal transport vesicles. (A) Axon of hippocampal neuron co-transfected at DIV7 with TAG-1–GFP and Caspr2–mCherry. Time-lapse images of axonal transport vesicles were acquired at 1 frame every 1.5 s for 220 s. (B–D) Corresponding kymographs showing overlapping trajectories of vesicles labeled for TAG-1–GFP (B) and Caspr2–mCherry (C). (D) Anterograde and retrograde events are underlined with yellow and blue lines, respectively, and the velocity measured for each transport event. (E) Time-lapse sequence showing a moving vesicle that contains both TAG-1–GFP and Caspr2–mCherry indicated with arrows. Scale bars: 10 μ m (A); 6 μ m (E). See also the corresponding Movie 1.

axon was clearly identified on the basis of its length, and was strongly enriched in transport vesicles by comparison with dendrites. In addition, live immunolabeling of neurofascin-186 was used to precisely localize the AIS after time-lapse recording (Fig. 5, blue). We found that most of the axonal transport vesicles were colabeled for Caspr2 and TAG-1 (Fig. 4E; Movie 1). Kymograph analysis of transport events indicated that double-labeled vesicles moved bi-directionally as illustrated in Fig. 4B–D. In neurons that were transfected with TAG-1–GFP alone, we observed that labeled vesicles were mostly axonally transported in the retrograde direction with a maximal velocity (V_m) of 0.34–0.64 μ m/s (Table S1; Fig. 5A). In neurons that were transfected with Caspr2–mCherry alone, labeled vesicles were transported in the anterograde and retrograde directions with a V_m of 0.66–1.46 and 0.75–0.95 μ m/s, respectively (Table S1; Fig. 5B,C). The vesicular transport of Caspr2–mCherry was similar to that described previously for Caspr2–GFP (Bel et al., 2009). Of note, mCherry was fused at the C-terminal of Caspr2 and did not perturb its transport by comparison with GFP, which was inserted downstream the signal peptide. Finally, when double-transfected for Caspr2 and TAG-1, some neurons exhibited bidirectional transport of colabeled vesicles (Fig. 5D; Table S1), whereas in most neurons, the vesicular transport was mainly observed in the retrograde direction with a velocity of 0.35–0.62 μ m/s (Fig. 5E,F; Movie 2, Table S1). Some vesicles were observed moving retrogradely starting from the axonal growth cone (Movie 3) and may result from endocytosis as previously described (Bel et al., 2009). The retrograde axonal transport may indicate a very dynamic renewal of Caspr2 and TAG-1 at the axonal membrane.

In conclusion, Caspr2 and TAG-1 are sorted within the same axonal vesicles even if they are distributed to distinct locations along the axon. Thus, we hypothesize that these proteins may be differentially distributed to AIS or axon according to diffusion and/or trapping mechanisms.

The cytoplasmic tail of Caspr2 promotes the recruitment of the MAGuK protein MPP2 at the AIS

Next, we addressed the role of the cytoplasmic tail of Caspr2 and whether it may contain a motif for its recruitment to the axon. We generated a Nr–Caspr2cyt construct (Fig. 6A) with the cytoplasmic tail of Caspr2 fused to the reporter NrCAM-Ig previously described in Falk et al., (2004). Strikingly, we observed that this chimera (green) was strongly enriched at the AIS surface of DIV8 hippocampal neurons double-stained for ankyrinG (blue) (Fig. 6B,C), with an AIS:axon ratio of 4 ± 0.6 (Fig. 6G). Deletion of the C-terminal region or the PDZ-binding motif induced relocalization all along the axon with an AIS:axon ratio of 1.5 ± 0.3 and 1.6 ± 0.2 , respectively (Fig. 6E–G). We also observed that deletion of the 4.1B-binding site induced a significant decrease in the AIS enrichment. The Δ 4.1B mutant displayed an AIS:axon ratio of 2.1 ± 0.3 (Fig. 6D,G). These results indicate that the cytoplasmic region of Caspr2 contains determinants for its AIS enrichment, namely, the 4.1B- and PDZ-binding domains. However, in the context of full-length Caspr2, its ectodomain exerts a dominant effect promoting axonal distribution.

The PDZ-binding domain of Caspr2 is a type II binding sequence and does not interacting with type I PSD-93 or PSD-95 as reported for Kv1 channels (Ogawa et al., 2008). It was reported to associate with MAGuK proteins of the CASK and MPP2 family in GST pull-down assays (Horresh et al., 2008). Hence, we generated CASK–mCherry and MPP2–mCherry constructs and observed that these MAGuK proteins were strongly recruited to the plasma

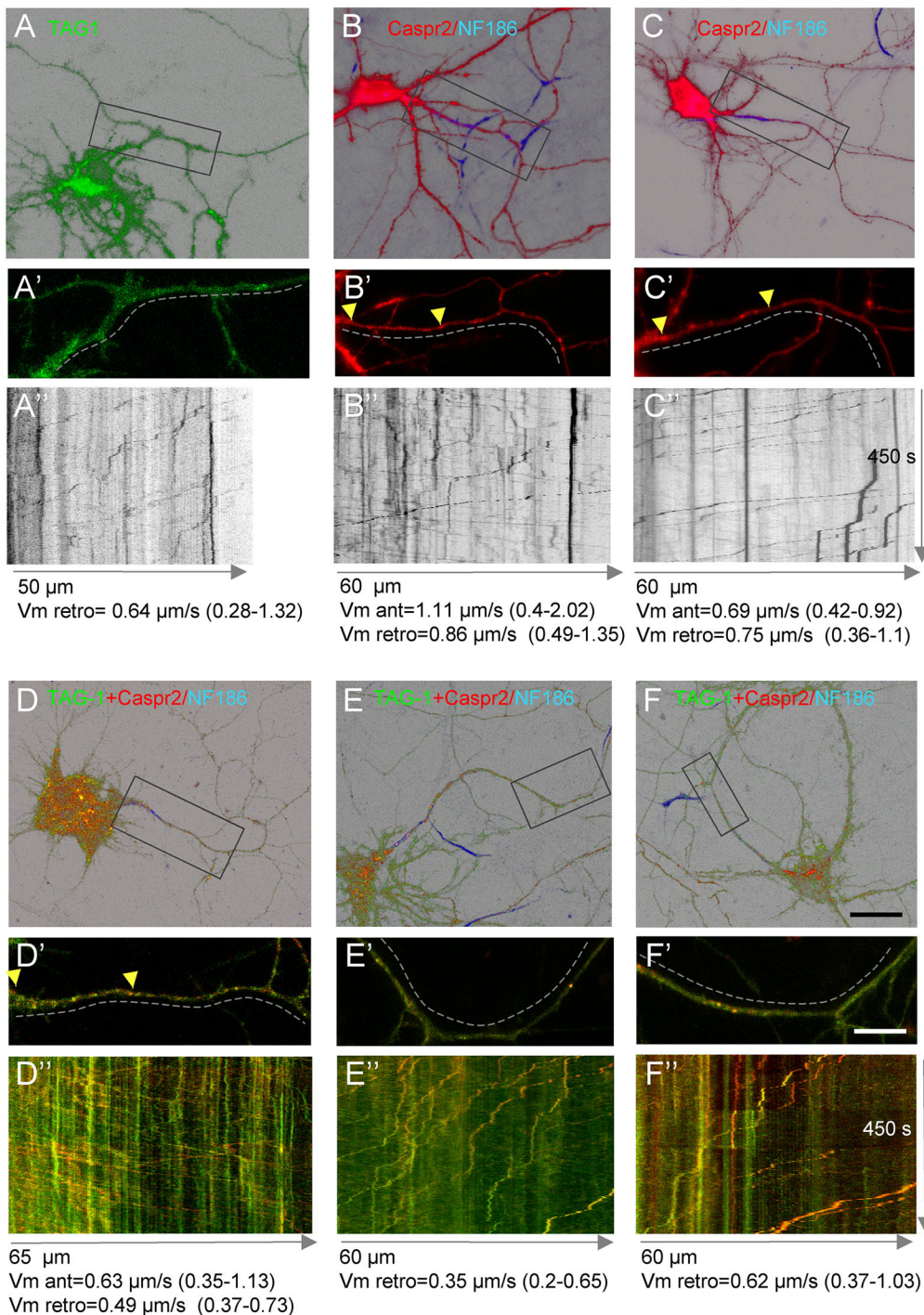


Fig. 5. Hippocampal neurons showing different types of axonal transport events for TAG-1-GFP and Caspr2-mCherry vesicles.

Hippocampal neurons were transfected at DIV7 with TAG-1-GFP (A), Caspr2-mCherry (B,C) or double-transfected with both CAMs (D-F). Time-lapse images of axonal transport vesicles were acquired at 1 frame every 1.5 s for 450 s. (B-F) Live immunostaining with Alexa-Fluor-647-coupled anti-neurofascin-186 was performed to determine the AIS location (blue), as indicated with arrowheads in B'-D'. The insets in A'-F' show the scanned axonal regions. Underlined axonal segments were used for kymograph analysis (axonal length in x-axis, time in y-axis) (A''-F'') and the maximal velocity (V_m) was determined for anterograde (ant) and retrograde (retro) events. Note that in A'', E'' and F'', transport events were mostly in the retrograde direction for TAG-1-GFP (A''), Caspr2-mCherry (C'') and double-labeled vesicles (E'', F''). In some neurons, bidirectional events were detected for Caspr2-mCherry and double-labeled vesicles (B'', D''). See also Movie 2 showing retrograde transport of double-labeled vesicles. Scale bar: 20 μm (F); 10 μm (F').

membrane when co-transfected with Nr-Caspr2cyt in HEK cells, as shown for MPP2 (Fig. 7A). MPP2 was not recruited to the plasma membrane by Nr-Caspr2cyt with a deletion of its PDZ-binding domain (Fig. 7B). Next, we performed co-immunoprecipitation experiments after transfection in HEK cells. Caspr2 was precipitated with MPP2 (Fig. 7D-G, last lane) and with CASK (data not shown). Nr-Caspr2cyt was even more strongly precipitated by MPP2 (Fig. 7D-G, first lane). As expected, co-immunoprecipitation of Nr-Caspr2cyt with MPP2 was prevented by deletion of its C-terminal region or PDZ-binding domain (Fig. 7D-G, ΔC and ΔZ). Deletion of the 4.1B-binding site also significantly inhibited co-immunoprecipitation with MPP2 (Fig. 7D-G, $\Delta\text{4.1}$), indicating that

it may participate in stabilizing the interaction with the MAGuK protein.

To examine whether MAGuK proteins could be recruited to the AIS, hippocampal neurons were co-transfected with Caspr2, Caspr2 Δ2 , or Nr-Caspr2cyt and MPP2-mCherry (Fig. 8). When co-transfected with full-length Caspr2, MPP2-mCherry was homogeneously distributed in the cytoplasm of hippocampal neurons and did not colocalize with Caspr2 along the axon (Fig. 8A). Strikingly, MPP2-mCherry became recruited to the AIS when co-transfected with Caspr2 Δ2 (Fig. 8B,B') or Nr-Caspr2cyt (Fig. 8C,D,D'). In addition, MPP2-mCherry colocalized with Nr-Caspr2cyt in intracellular vesicles (Fig. 8D'') in accordance

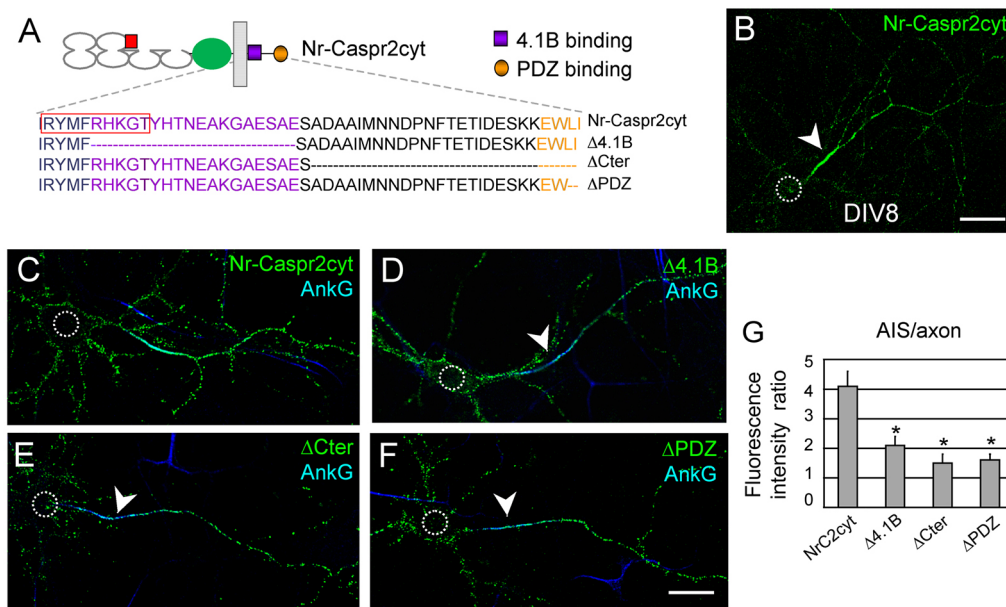


Fig. 6. The Caspr2 cytoplasmic region promotes enrichment at the AIS. (A) The Nr-Caspr2cyt reporter construct contains the Caspr2 transmembrane and cytoplasmic regions fused to the NrCAM signal peptide and Ig domains, tagged with HA and GFP. The sequence of the cytoplasmic tail of Caspr2 contains a 4.1B-binding region (purple), an endocytosis motif (red box) and a PDZ-binding motif (orange). Deletions in Δ4.1B, ΔCter and ΔPDZ mutants are indicated. (B–F) Hippocampal neurons transfected at DIV7 with the reporter Nr-Caspr2cyt constructs and surface labeled with anti-HA mAb (green). Double-staining was performed for the AIS marker ankyrinG (blue). The soma is indicated with circles and AIS highlighted with arrowheads. Note that only Nr-Caspr2cyt is highly enriched at the AIS (B,C). Scale bars: 20 μm (B); 10 μm (F). (G) AIS:axon ratios of fluorescence intensity measured for Nr-Caspr2cyt (NrC2cyt) and the deleted constructs Δ4.1B, ΔCter and ΔPDZ (means±s.e.m.; $n=10$). * $P<0.05$ by comparison with Nr-Caspr2cyt (ANOVA).

with endocytosis mediated by the Caspr2 cytoplasmic tail (Bel et al., 2009).

The fact that, upon transfection of Caspr2, MPP2 was not recruited to the AIS or along the axon, indicated that an outside-in mechanism might regulate this association. The C-terminal region of Caspr2 contains several consensus sites for phosphorylation by the casein kinase 2 (CK2) (Thr1319, Thr1321 and Ser1325; NetPhos 3.1 prediction server) that might regulate the PDZ-binding site of Caspr2. We generated several constructs of Nr-Caspr2cyt as shown in Fig. 7C including mutating Thr1319 and Thr1321 into alanine (TTAA) or glutamate (TTEE) residues and mutation of Ser1325 to a glutamate residue (SE). When transfected into hippocampal neurons, all these mutated constructs were recruited to the AIS (not shown). In addition, co-immunoprecipitation experiments did not show any effect of these mutations on MPP2 binding (Fig. 7D–G). Thus, we could not identify a phosphorylation mechanism possibly regulating the recruitment of Caspr2 at the AIS through its interaction with a MAGuK protein. Alternatively, we showed that the 4.1B-binding domain plays a modulating role on this interaction.

We examined whether the recruitment of Nr-Caspr2cyt and MPP2 at the AIS may be correlated with the concentration of Kv1 channels at that site. Hippocampal neurons were co-transfected with Nr-Caspr2cyt and MPP2. The mean AIS:axon ratio of fluorescence intensity was 3.10 ± 0.17 for Nr-Caspr2cyt, 3.09 ± 0.56 for MPP2, and 2.94 ± 0.32 for Kv1.2 (Fig. S2). The individual values ($n=18$) were plotted showing that the AIS:axon ratios for both Nr-Caspr2cyt and MPP2 were correlated with that of the Kv1.2 channels. This result indicated that MPP2 can be recruited by the scaffold associated with the Kv1.2 complex.

Taken together, these data indicate that MPP2 could be trapped at the AIS through its association with the Caspr2 PDZ-binding domain. This MPP2 interaction appears to be downregulated in full-length Caspr2. An important point will be to determine which

endogenous MAGuK protein of the MPP2 family could be present at the AIS.

DISCUSSION

The precise sub-compartmental profile of Kv1 channels at AIS and along axons is critical for the shaping of neuronal signaling. In the present study, we showed that two CAMs associated with Kv1, TAG-1 and Caspr2, are distinctly targeted along the axon in hippocampal neurons. TAG-1 strongly colocalizes with Kv1.2 channels at the AIS whereas Caspr2 is evenly distributed along the axon, in contrast to their colocalization at juxtaparanodes. Live imaging of Caspr2 and TAG-1 vesicular transport revealed that they are sorted together in the same axonal transport vesicles. Thus, we hypothesize that their differential distribution may result from diffusion and/or trapping mechanisms induced by selective partnerships. We identified two molecular determinants of Caspr2 that regulate its axonal positioning. First, we showed that deletion of the LNG2-EGF1 extracellular modules in Caspr2Δ2 induces its restricted localization at the AIS and strengthened its association with TAG-1. Second, we demonstrated that the cytoplasmic tail of Caspr2 contains a PDZ-binding site that elicits AIS enrichment and recruitment of the MAGuK protein MPP2. Hence, the distribution of Caspr2 and TAG-1 at the AIS versus all along the axon may be regulated and participate in the strategic function of the Kv1 complex along axons.

We previously showed that Caspr2 is both inserted at the axonal and somatodendritic membranes (Bel et al., 2009). The selective endocytosis of Caspr2 in the somatodendritic compartment further promotes its polarized expression at the axonal surface (Bel et al., 2009). The distinct distribution of TAG-1 and Caspr2 at the AIS and along the axon could have been due to their sorting in dedicated vesicles that would then fuse to specific domains. However, in live-cell imaging experiments, we observed that TAG-1 and Caspr2

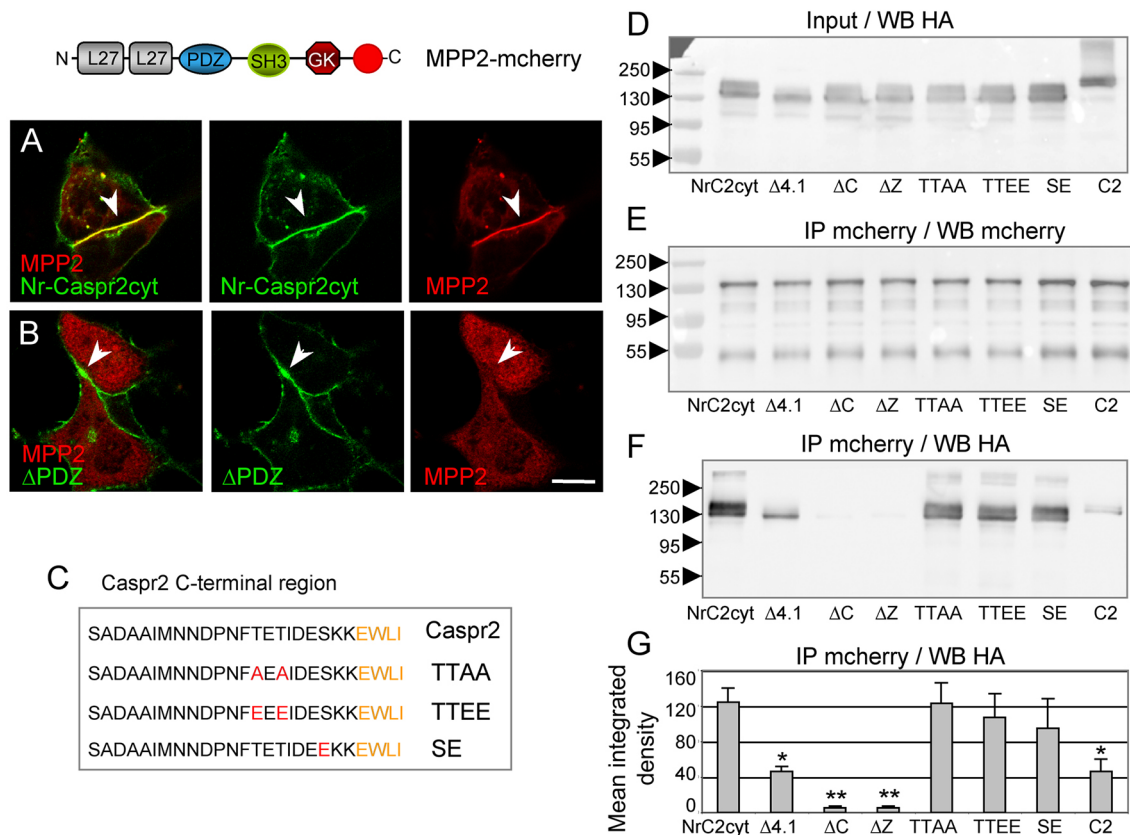


Fig. 7. The PDZ-protein MPP2 interacts with Caspr2 in transfected HEK cells. (A,B) HEK cells were co-transfected with MPP2–mCherry and Nr–Caspr2cyt (A) or Δ PDZ (B) constructs. Cells were fixed with methanol and the fluorescence was directly imaged in confocal sections. The cytoplasmic tail of Caspr2 induced the recruitment of MPP2 at the cell membrane (arrowheads in A) and deletion of the PDZ-binding regions prevented its recruitment (arrowheads in B). Scale bar: 5 μ m. (C) Nr–Caspr2cyt constructs were generated with mutations (indicated in red) of the Thr and Ser-phosphorylation sites in the C-terminal region upstream the PDZ-binding sequence (orange). Thr1319 and Thr1321 were mutated to alanine residues (TTAA) or glutamate residues (TTEE), or the Ser1325 was mutated into a glutamate residue (SE). (D–F) HEK cells were co-transfected with MPP2–mCherry and HA-tagged full-length Caspr2 or Nr–Caspr2cyt mutants. Cells were lysed and the supernatants analyzed for expression of Caspr2 and Nr–Caspr2cyt mutants by western blotting (WB) for HA (D, input). Immunoprecipitation (IP) was performed using rabbit anti-mCherry antibody and the immunoprecipitates (IP) analyzed by western blotting for MPP2–mCherry (E) and HA-tagged constructs (F). Caspr2 (C2) and Nr–Caspr2cyt (NrC2cyt) constructs were co-immunoprecipitated with MPP2. Mutants with deletion of the C-terminal (Δ C) or PDZ-binding (Δ Z) domain were not co-precipitated, and mutations of the Ser- or Thr-phosphorylation sites in the C-terminal region had no effect. Deletion of the 4.1B-binding (Δ 4.1) region strongly reduced the interaction with MPP2. The experiments were performed in triplicate. Quantitative analysis of co-immunoprecipitated proteins was performed using the ImageJ software and expressed as a mean \pm s.e.m. percentage of the Nr–Caspr2cyt value. * P <0.05; ** P <0.01 by comparison with Nr–Caspr2cyt (ANOVA).

are colocalized in axonal transport vesicles. We noticed that both TAG-1 and Caspr2 are mostly transported in the retrograde direction. Hence, these proteins are not packaged into separate vesicles and their proper cell surface accumulation at different axonal sites may depend on diffusion-trapping mechanisms. The AIS is a zone of restricted diffusion for the lateral mobility of transmembrane proteins that are anchored to the ankyrin–spectrin–actin cytoskeleton, like neurofascin-186 and voltage-gated Na^+ channels (Jenkins and Bennett, 2001; Leterrier, 2016). This zone contains a high density of proteins that are anchored to cortical actin and act as a picket fence that restrains the diffusion of unanchored constituents (Winckler et al., 1999), such as GPI-anchored proteins like TAG-1. The limited diffusion of GPI-anchored proteins at the AIS may be also related to the periodic organization of the actin cytoskeleton recently revealed by super-resolution microscopy (Albrecht et al., 2016). In addition, the AIS is the site of a selective barrier for vesicles carrying dendritic cargoes that only enter into the base of the axon, before stopping and returning to the soma. In contrast, axonal cargo vesicles pass through the AIS and proceed to the distal axon (Al-Bassam et al., 2012; Petersen et al., 2014).

Here, we observed that both Caspr2 and TAG-1 vesicles are axonally transported through the AIS without impediment both in the anterograde and retrograde directions and we did not observe any fusion of vesicles within the AIS. Retrogradely moving vesicles were also observed starting from the axonal growth cone and likely result from endocytosis. In a previous paper (Bel et al., 2009), we reported that Caspr2 is strongly internalized in the somato-dendritic compartment by comparison with the axon. Since axons are highly ramified at DIV8, even if endocytosis occurred at a low rate, the multiple axonal tips might produce a number of retrogradely moving vesicles. The retrograde axonal transport suggests a very dynamic renewal of Caspr2 and TAG-1 at the axonal membrane.

TAG-1 is a GPI-anchored molecule, indicating that its ectodomain may drive its distribution at the AIS. As an Ig-CAM, TAG-1 displays a broad activity of binding and may associate with NrCAM or neurofascin-186 (Lustig et al., 1999), which are trapped at the AIS via an ankyrin-binding motif (Davis et al., 1996). However, we showed that the TAG-1-Ig construct is poorly enriched at the AIS when compared with full-length TAG-1, indicating

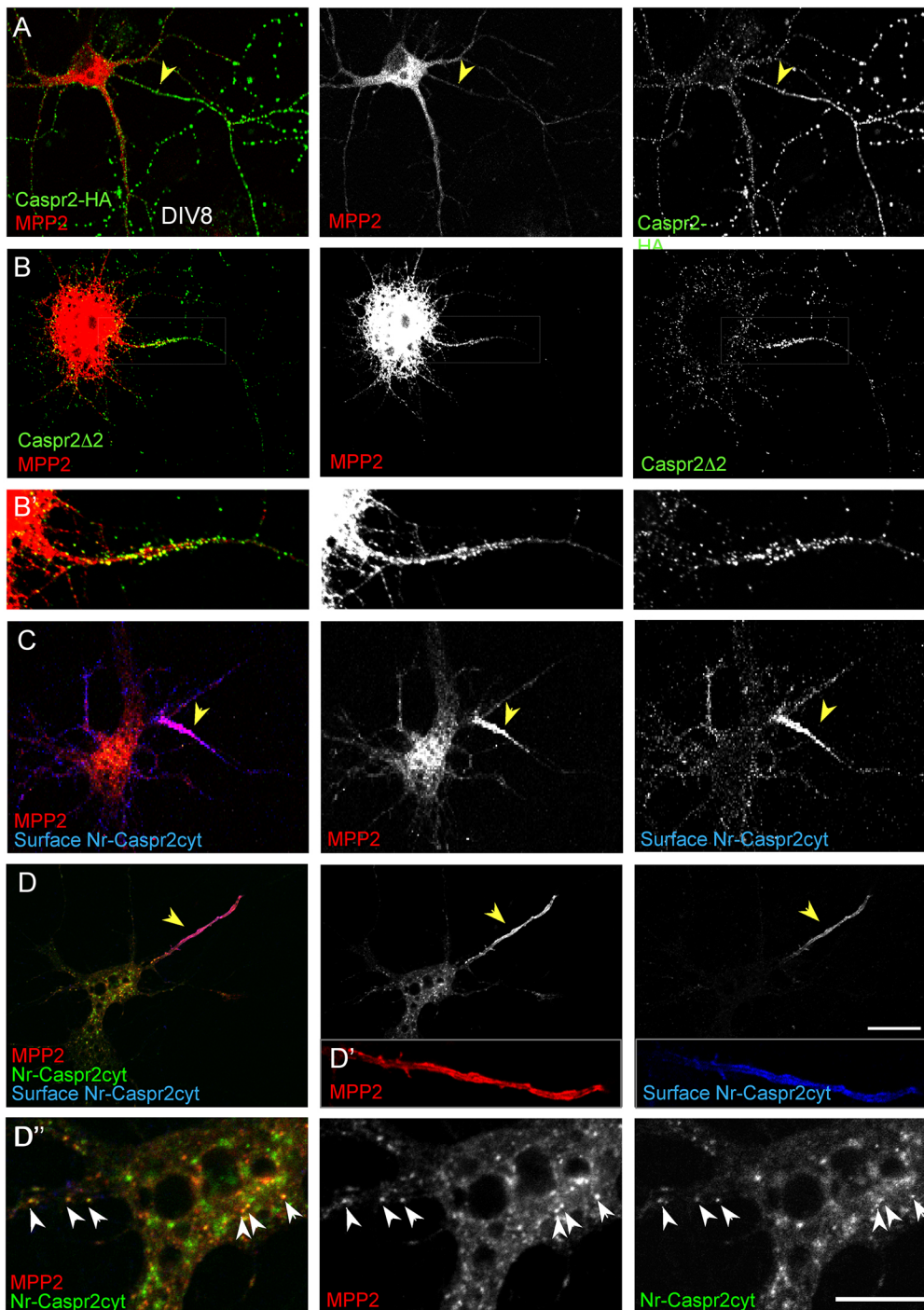


Fig. 8. The PDZ-protein MPP2 is recruited by the Caspr2 cytoplasmic tail at the AIS of hippocampal neurons. (A,B) Hippocampal neurons were co-transfected at DIV7 with MPP2–mCherry and full-length Caspr2 (A) or Caspr2 Δ 2 (B,B'). Neurons were surface labeled at DIV8 with anti-HA mAb (green) and fixed. The fluorescence for MPP2–mCherry was directly imaged (red). Note that MPP2 colocalized in clusters with Caspr2 Δ 2 at the AIS (arrowheads). (C,D) Hippocampal neurons were transfected with MPP2–mCherry and GFP-tagged Nr–Caspr2cyt. Cells were surface labeled for GFP (blue) and fixed. The fluorescence for MPP2–mCherry (red) and Nr–Caspr2cyt (green) was directly imaged. Note, that MPP2 strongly colocalized with Nr–Caspr2cyt at the AIS (yellow arrowheads in C,D) and in intracellular vesicles (white arrowheads in D''). Scale bar: 20 μ m (D), 10 μ m (D'').

that the conformation of the intact molecule is essential for its enrichment at the AIS, which may occur independently of NrCAM/neurofascin-186 binding. The extracellular domain of Caspr2 is implicated in its axonal versus AIS distribution. Deletion of the LNG2-EGF1 region induces the concentration of Caspr2 Δ 2 at the AIS. One hypothesis could be that these modules interact with a cis-partner that drives the distribution of Caspr2 all along the axon. Alternatively, given the overall organization of Caspr2, the LNG2-EGF1 deletion may induce a structural change favoring TAG-1 binding. The architecture of Caspr2 is composed of three lobes with the discoidin, LNG1 and LNG2 domains forming a large lobe, the fibrinogen and LNG3 a middle lobe, and LNG4 a small lobe (Lu

et al., 2016; Rubio-Marrero et al., 2016). In support of this second hypothesis, we showed that deletion of the LNG2-EGF1 modules of Caspr2 increases its cis-association with TAG-1 as analyzed using co-immunoprecipitation experiments from double-transfected HEK cells.

The cytoplasmic tail of Caspr2 contains a juxtamembrane 4.1B-binding sequence and a C-terminal PDZ type II-binding motif. We showed that deletion of each of these motifs decreases the AIS enrichment of the Caspr2 cytoplasmic tail reporter construct. Proteomic analysis had revealed that Caspr2 may interact with a set of scaffolding proteins including the MAGuKs MPP2 and CASK, and the multiple PDZ domain protein MUPP1 (Horresh

et al., 2008; Tanabe et al., 2015). Horresh et al. also reported that the association of Caspr2 with MPP2 requires its 4.1B- and PDZ-binding regions (Horresh et al., 2008). We showed here that Caspr2 could be co-immunoprecipitated with MPP2 or CASK from the lysate of co-transfected HEK cells. Deletion of the 4.1B-binding domain significantly decreases co-immunoprecipitation and also prevents the recruitment of MPP2 to the plasma membrane of HEK cells. In contrast, we did not see any effect of mutating the consensus sites for CK2 phosphorylation located in the C-terminal region. Interestingly, the Caspr2 cytoplasmic tail in the reporter construct and in the Caspr2 Δ 2 mutant strongly recruits MPP2–mCherry at the AIS of transfected hippocampal neurons. We noticed that in the context of Caspr2 full-length molecule, MPP2 was not recruited by the Caspr2 cytoplasmic tail at the AIS or along the axon. The ectodomain of Caspr2 contains the LNG2-EGF1 modules implicated in its axonal targeting, likely by regulating cis-interaction with CAMs. Hence, an outside-in mechanism might regulate the recruitment of a MAGuK protein and 4.1B to stabilize Caspr2 at the AIS depending on the neuronal cell type or cellular context. It would be interesting to elucidate whether any endogenous proteins of the MPP2 family may be present at the AIS. MPP2 is a MAGuK protein that contains two L27 domains belonging to a subfamily which also contains Varicose, a component of *Drosophila* septate junctions that binds neuexin IV, the homolog of Caspr and Caspr2 (Laval et al., 2008; Wu et al., 2007). CASK, which contains a calmodulin kinase domain and binds neuexin, is implicated in synaptic protein targeting (Hsueh, 2006). Caspr2 has been also reported to interact with MUPP1, which may play a role at the post-synapse (Krapivinsky et al., 2004; Tanabe et al., 2015). To our knowledge, none of these scaffolding proteins have been identified at the AIS and we were not able to detect MPP2 or CASK at this axonal sub-region using available commercial antibodies (data not shown).

The AIS diversity may reflect the physiological properties of the different neuronal cell types. In addition, the AIS may be a dynamic unit regulating intrinsic excitability of neurons during homeostatic plasticity or in pathological conditions (Kuba et al., 2010). Indeed, the position of AIS moves distally in hippocampal neurons after depolarization, and this movement correlates with change in current threshold for spike firing (Grubb and Burrone, 2010). We hypothesize that the AIS distribution of the Kv1 complex may be regulated depending on the neuronal cell type, differentiation stage or activity to fine-tune neuronal excitability. During the maturation of cultured hippocampal neurons, the Nav1.2 channels are recruited to the AIS shortly after ankyrinG at around DIV3, while the Kv1 channels begin to concentrate at DIV10 at that site (Sanchez-Ponce et al., 2012). TAG-1 is enriched at the AIS at DIV14, as observed for Kv1 channels. Since several CAMs associated with the Kv1 channels, including Caspr2 and LGI1, are implicated in genetic or autoimmune psychiatric diseases (Lai et al., 2010), it will be important to study whether their distribution at the AIS may provide clues on neuronal excitability in physiological and pathological conditions.

MATERIALS AND METHODS

Constructs

The pCDNA3-Caspr2-HA construct encodes human Caspr2 with the HA epitope inserted downstream of the signal peptide between the residues Trp26 and Thr27 (Bel et al., 2009). The Caspr2–HA deletion constructs, Caspr2 Δ 1 (Δ 32–361), Caspr2 Δ 2 (Δ 362–600), Caspr2 Δ 3 (Δ 600–950), Caspr2 Δ 4 (Δ 955–1169) were as described previously (Pinatel et al., 2015). The NrCAM–Caspr2cyt construct was generated by insertion of the Caspr2 transmembrane and cytoplasmic regions downstream the signal

peptide and Ig domains of NrCAM, and is tagged with HA and GFP (Falk et al., 2004). NrCAM–GFP, TAG-1-Fc, TAG-1-Ig-Fc and neurofascin-186–HA were as described previously (Falk et al., 2004; Labasque et al., 2011). Nr-Caspr2cyt constructs with deletions of the binding site for 4.1B (Δ 1288–1305), the PDZ-binding domain (stop at residue 1330) or the C-terminal region (stop codon at residue 1306) were generated. The human TAG-1–GFP and Caspr2–GFP constructs with GFP downstream of the signal peptide were as described previously (Bel et al., 2009; Pinatel et al., 2015). The human TAG-1–GFP deletion constructs were generated by PCR amplification from the previously described TAG-1-Ig and TAG-1-Fn constructs (Tzamourakas et al., 2007), and were inserted in the XhoI/ HindIII sites of a pEGFP-C1 plasmid vector modified to contain the signal peptide of TAG-1 upstream of GFP. Caspr2–mCherry, with mCherry at the C-terminus, was generated by insertion into the EcoRI–BamHI sites of pmCherry-N1. The coding sequence of human CASK and MPP2 were obtained from OriGene (Rockville, USA) and inserted into the EcoRI–BamHI sites of pmCherry-N1 vector. PCR amplified products were verified by sequencing (Genewiz, Takeley, GB).

Antibodies and immunofluorescence staining

The rat anti-HA mAb (clone 3F10, ref. 11867423001) was purchased from Roche (Meylan, France), the goat anti-GFP antibody (ab5450) from abcam (Paris, France), the rabbit anti-GFP antibody (A11122) from Molecular Probes (ThermoFisher, Courtaboeuf, France), the rabbit anti-RFP (anti-mCherry) antibody from Rockland (Limerick, USA), the rabbit anti-TAG-1 antibody (ABN1379) from Millipore (MerckMillipore, Fontenay sous Bois, France). The mouse anti-ankyrinG (N106/36), anti-CASK (clone K56A/50), and anti-neurofascin186 (clone A12/18) mAbs were obtained from the UC Davis/NIH NeuroMab facility. The mouse anti-TAG-1 1C12 mAb and the rabbit anti-Caspr2 antiserum were as previously described (Bel et al., 2009; Traka et al., 2003). Anti-Caspr2 antibodies from limbic encephalitis patients were characterized previously (Pinatel et al., 2015). Alexa Fluor 488-, 568- and 647-conjugated secondary antibodies were obtained from Molecular Probes (ThermoFisher). Immunostaining for Caspr2–HA, Caspr2–GFP and TAG-1–GFP was performed on live cells with antibodies against HA or GFP, diluted 1:1000 in culture medium, for 30–60 min. Cells were fixed with 4% paraformaldehyde in PBS for 10 min and permeabilized with 0.1% Triton X-100 for 10 min. Immunofluorescence staining was performed using mouse anti-ankyrinG (1:100) antibodies, and with secondary antibodies diluted in PBS containing 3% bovine serum albumin. After washing in PBS, cells were mounted in Mowiol (Calbiochem, MerckMillipore). The dilution of primary antibodies used for immunofluorescence staining is indicated in Table S2.

Cell culture

Cell culture media and reagents were from Gibco (ThermoFisher). HEK-293 cells (ATCC, Teddington, UK) were grown in Dulbecco's modified Eagle's medium (DMEM) containing 10% fetal calf serum, and were transiently transfected using jet PEI (Polyplus transfection, Ozyme, St Quentin en Yvelines, France). Primary hippocampal cell cultures were from embryonic day 18 Wistar rats. Hippocampi were collected in Hanks' balanced salt solution, dissociated with trypsin and plated at a density of 1.2×10^5 cells/cm² on poly-L-lysine-coated coverslips. The hippocampal neurons were cultured in Neurobasal supplemented with 2% B-27, 1% penicillin-streptomycin and 0.3% glutamine in a humidified atmosphere containing 5% CO₂ at 37°C. Hippocampal neurons were transfected with Lipofectamine 2000 (Invitrogen, ThermoFisher) at DIV7 or DIV14. All animal experiments were carried out according to the animal care and experimentation committee rules approved by CNRS.

Confocal microscopy and image analysis

Image acquisition was performed on a Zeiss (Carl Zeiss France, Marly le Roi) laser-scanning microscope equipped with 63 \times 1.32 NA oil-immersion objective. Images of GFP or mCherry or Alexa-Fluor-stained cells were obtained using the 488 nm band of an Argon laser and the 568 nm and 647 nm bands of a solid-state laser for excitation. Fluorescence images were collected automatically with an average of two-frame scans. Quantitative image analysis was performed by using ImageJ on confocal sections (20

neurons in each condition). The fluorescence intensity was measured in two regions of interest (the ankyrinG-positive AIS and the axon) using identical confocal parameters. The fluorescence intensity profiles were obtained by using Zen software (Zeiss). Statistical analysis was performed with ANOVA.

Imaging vesicle transport

Coverslips with neurons were loaded into a sealed heated chamber in imaging medium (Hank's balanced salt solution pH 7.2 with 10 mM HEPES and 0.6% glucose). Recordings were made 18 h after transfection. The axons were selected on the basis of their much greater length by comparison with dendrites. Live immunostaining using Alexa-Fluor-647-coupled anti-neurofascin-186 was performed after recordings to detect the AIS. Vesicle transport was imaged using Zeiss laser-scanning microscope equipped with 63×1.32 NA oil-immersion objective and 37°C heating chamber. Dual-color recordings were acquired by using simultaneous excitation with 488 (2–4%) and 561 lasers (1–2%), and a GaSP PMT1 detector for 499–551 nm and PMT2 detector for 569–735 nm (562×240 pixels, average 2, open pinhole, 1.5 s scanning time, streamed time-lapse recording during 4–8 min). Kymographs were generated by using ImageJ software and were contrast inverted so that the fluorescent vesicles corresponded to dark lines. Overlapping transport events were analyzed and the velocity measured for each transport event.

Western blot and immunoprecipitation

HEK cells were co-transfected with Caspr2–HA or NrCAM–Caspr2_{cyt} constructs and CASK–mCherry or MPP2–mCherry, or with Caspr2–HA deletion constructs and TAG-1–GFP. Cells were lysed for 30 min on ice with 50 mM Tris, pH 7.5, 1% NP-40, 10 mM MgCl₂ and protease inhibitors, centrifuged at 4°C for 15 min at 15,000 rpm. After preclearing for 1 h at 4°C with protein A-Sepharose, supernatants were immunoprecipitated overnight at 4°C with protein A-Sepharose coated with rabbit anti-mCherry antibody (2 µg), or rabbit anti-Caspr2 antiserum (2 µl). The beads were washed twice with 50 mM Tris-HCl pH 7.4, 150 mM NaCl and 1% NP-40, twice in 50 mM Tris-HCl, 150 mM NaCl and twice in 50 mM Tris-HCl. Immune precipitates were analyzed by immunoblotting with rat anti-HA and rabbit anti-mCherry, or rabbit anti-Caspr2 and rabbit anti-TAG-1 antibodies. Blots were developed using the ECL chemiluminescent detection system (Roche). Quantitative analysis of co-immunoprecipitated proteins was performed by using the ImageJ software.

Acknowledgements

We wish to thank Marie-Pierre Blanchard of the CRN2M imaging core facility for help with time-lapse recording and image analysis. We are grateful to Laurence Goutebroze and Christophe Leterrier for helpful discussions. We thank the UC Davis/NIH NeuroMab facility.

Competing interests

The authors declare no competing or financial interests.

Author contributions

Conceptualization: D.P., B.H., C.F.; Methodology: B.H., C.F.; Validation: D.P., M. Saint-Martin, N.N., C.F.; Formal analysis: C.F.; Investigation: D.P., B.H., M. Saint-Martin, C.F.; Resources: M. Savvaki, D.K., C.F.; Writing - original draft: C.F.; Writing - review & editing: D.P., N.N., M. Savvaki, D.K., C.F.; Supervision: C.F.; Project administration: C.F.; Funding acquisition: C.F.

Funding

This work was supported by the Fondation pour l'Aide à la Recherche sur la Sclérose en Plaques (ARSEP) to C.F.-S. and D.K.

Supplementary information

Supplementary information available online at <http://jcs.biologists.org/lookup/doi/10.1242/jcs.202267.supplemental>

References

Al-Bassam, S., Xu, M., Wandless, T. J. and Arnold, D. B. (2012). Differential trafficking of transport vesicles contributes to the localization of dendritic proteins. *Cell Rep.* **2**, 89–100.

- Albrecht, D., Winterlood, C. M., Sadeghi, M., Tschager, T., Noé, F. and Ewers, H. (2016). Nanoscopic compartmentalization of membrane protein motion at the axon initial segment. *J. Cell Biol.* **215**, 37–46.
- Bel, C., Oguievetskaia, K., Pitaval, C., Goutebroze, L. and Faivre-Sarrailh, C. (2009). Axonal targeting of Caspr2 in hippocampal neurons via selective somatodendritic endocytosis. *J. Cell Sci.* **122**, 3403–3413.
- Buttermore, E. D., Dupree, J. L., Cheng, J., An, X., Tessarollo, L. and Bhat, M. A. (2011). The cytoskeletal adaptor protein band 4.1B is required for the maintenance of paranodal axoglial septate junctions in myelinated axons. *J. Neurosci.* **31**, 8013–8024.
- Cifuentes-Diaz, C., Chareyre, F., Garcia, M., Devaux, J., Carnaud, M., Levasseur, G., Niwa-Kawakita, M., Harroch, S., Girault, J.-A., Giovannini, M. et al. (2011). Protein 4.1B contributes to the organization of peripheral myelinated axons. *PLoS ONE* **6**, e25043.
- Davis, J. Q., Lambert, S. and Bennett, V. (1996). Molecular composition of the node of Ranvier: identification of ankyrin-binding cell adhesion molecules neurofascin (mucin+/third FNIII domain-) and NrCAM at nodal axon segments. *J. Cell Biol.* **135**, 1355–1367.
- Devaux, J. J., Kleopa, K. A., Cooper, E. C. and Scherer, S. S. (2004). KCNQ2 is a nodal K⁺ channel. *J. Neurosci.* **24**, 1236–1244.
- Dufflocq, A., Chareyre, F., Giovannini, M., Couraud, F. and Davenne, M. (2011). Characterization of the axon initial segment (AIS) of motor neurons and identification of a para-AIS and a juxtapara-AIS, organized by protein 4.1B. *BMC Biol.* **9**, 66.
- Einheber, S., Meng, X., Rubin, M., Lam, I., Mohandas, N., An, X., Shrager, P., Kissil, J., Maurel, P. and Salzer, J. L. (2013). The 4.1B cytoskeletal protein regulates the domain organization and sheath thickness of myelinated axons. *Glia* **61**, 240–253.
- Falk, J., Thoumine, O., Dequidt, C., Choquet, D. and Faivre-Sarrailh, C. (2004). NrCAM coupling to the cytoskeleton depends on multiple protein domains and partitioning into lipid rafts. *Mol. Biol. Cell* **15**, 4695–4709.
- Grubb, M. S. and Burrone, J. (2010). Activity-dependent relocation of the axon initial segment fine-tunes neuronal excitability. *Nature* **465**, 1070–1074.
- Horresh, I., Poliak, S., Grant, S., Bredt, D., Rasband, M. N. and Peles, E. (2008). Multiple molecular interactions determine the clustering of Caspr2 and Kv1 channels in myelinated axons. *J. Neurosci.* **28**, 14213–14222.
- Horresh, I., Bar, V., Kissil, J. L. and Peles, E. (2010). Organization of myelinated axons by Caspr and Caspr2 requires the cytoskeletal adapter protein 4.1B. *J. Neurosci.* **30**, 2480–2489.
- Hsueh, Y.-P. (2006). The role of the MAGUK protein CASK in neural development and synaptic function. *Curr. Med. Chem.* **13**, 1915–1927.
- Inda, M. C., DeFelipe, J. and Munoz, A. (2006). Voltage-gated ion channels in the axon initial segment of human cortical pyramidal cells and their relationship with chandelier cells. *Proc. Natl. Acad. Sci. USA* **103**, 2920–2925.
- Irani, S. R., Bien, C. G. and Lang, B. (2010). Autoimmune epilepsies. *Curr. Opin. Neurol.* **24**, 146–153.
- Jenkins, S. M. and Bennett, V. (2001). Ankyrin-G coordinates assembly of the spectrin-based membrane skeleton, voltage-gated sodium channels, and L1 CAMs at Purkinje neuron initial segments. *J. Cell Biol.* **155**, 739–746.
- King, A. N., Manning, C. F. and Trimmer, J. S. (2014). A unique ion channel clustering domain on the axon initial segment of mammalian neurons. *J. Comp. Neurol.* **522**, 2594–2608.
- Kole, M. H. P. and Stuart, G. J. (2012). Signal processing in the axon initial segment. *Neuron* **73**, 235–247.
- Krapivinsky, G., Medina, I., Krapivinsky, L., Gapon, S. and Clapham, D. E. (2004). SynGAP-MUFP1-CaMKII synaptic complexes regulate p38 MAP kinase activity and NMDA receptor-dependent synaptic AMPA receptor potentiation. *Neuron* **43**, 563–574.
- Kuba, H., Oichi, Y. and Ohmori, H. (2010). Presynaptic activity regulates Na⁺ channel distribution at the axon initial segment. *Nature* **465**, 1075–1078.
- Labasque, M., Devaux, J. J., Lévêque, C. and Faivre-Sarrailh, C. (2011). Fibronectin type III-like domains of neurofascin-186 protein mediate gliomedin binding and its clustering at the developing nodes of Ranvier. *J. Biol. Chem.* **286**, 42426–42434.
- Lai, M., Huijbers, M. G. M., Lancaster, E., Graus, F., Bataller, L., Balice-Gordon, R., Cowell, J. K. and Dalmau, J. (2010). Investigation of LGI1 as the antigen in limbic encephalitis previously attributed to potassium channels: a case series. *Lancet Neurol.* **9**, 776–785.
- Lancaster, E., Huijbers, M. G. M., Bar, V., Boronat, A., Wong, A., Martínez-Hernández, E., Wilson, C., Jacobs, D., Lai, M., Walker, R. W. et al. (2011). Investigations of caspr2, an autoantigen of encephalitis and neuromyotonia. *Ann. Neurol.* **69**, 303–311.
- Laval, M., Bel, C. and Faivre-Sarrailh, C. (2008). The lateral mobility of cell adhesion molecules is highly restricted at septate junctions in *Drosophila*. *BMC Cell Biol.* **9**, 38.
- Leterrier, C. (2016). The axon initial segment, 50 years later: a nexus for neuronal organization and function. *Curr. Top. Membr.* **77**, 185–233.
- Lu, Z., Reddy, M. V., Liu, J., Kalichava, A., Liu, J., Zhang, L., Chen, F., Wang, Y., Holthausen, L. M., White, M. A. et al. (2016). Molecular Architecture of

- Contactin-associated Protein-like 2 (CNTNAP2) and Its Interaction with Contactin 2 (CNTN2). *J. Biol. Chem.* **291**, 24133–24147.
- Lustig, M., Sakurai, T. and Grumet, M. (1999). Nr-CAM promotes neurite outgrowth from peripheral ganglia by a mechanism involving axonin-1 as a neuronal receptor. *Dev. Biol.* **209**, 340–351.
- Ogawa, Y., Horresh, I., Trimmer, J. S., Bredt, D. S., Peles, E. and Rasband, M. N. (2008). Postsynaptic density-93 clusters Kv1 channels at axon initial segments independently of Caspr2. *J. Neurosci.* **28**, 5731–5739.
- Ogawa, Y., Oses-Prieto, J., Kim, M. Y., Horresh, I., Peles, E., Burlingame, A. L., Trimmer, J. S., Meijer, D. and Rasband, M. N. (2010). ADAM22, a Kv1 channel-interacting protein, recruits membrane-associated guanylate kinases to juxtaparanodes of myelinated axons. *J. Neurosci.* **30**, 1038–1048.
- Pan, Z., Kao, T., Horvath, Z., Lemos, J., Sul, J. Y., Cranstoun, S. D., Bennett, V., Scherer, S. S. and Cooper, E. C. (2006). A common ankyrin-G-based mechanism retains KCNQ and NaV channels at electrically active domains of the axon. *J. Neurosci.* **26**, 2599–2613.
- Petersen, J. D., Kaech, S. and Banker, G. (2014). Selective microtubule-based transport of dendritic membrane proteins arises in concert with axon specification. *J. Neurosci.* **34**, 4135–4147.
- Pinatel, D., Hivert, B., Boucraut, J., Saint-Martin, M., Rogemond, V., Zoupi, L., Karagogeos, D., Honnorat, J. and Faivre-Sarrailh, C. (2015). Inhibitory axons are targeted in hippocampal cell culture by anti-Caspr2 autoantibodies associated with limbic encephalitis. *Front. Cell Neurosci.* **9**, 265.
- Poliak, S., Salomon, D., Elhanany, H., Sabanay, H., Kiernan, B., Pevny, L., Stewart, C. L., Xu, X., Chiu, S.-Y., Shrager, P. et al. (2003). Juxtaparanodal clustering of Shaker-like K⁺ channels in myelinated axons depends on Caspr2 and TAG-1. *J. Cell Biol.* **162**, 1149–1160.
- Rama, S., Zbili, M. and Debanne, D. (2015). Modulation of spike-evoked synaptic transmission: the role of presynaptic calcium and potassium channels. *Biochim. Biophys. Acta* **1853**, 1933–1939.
- Rubio-Marrero, E. N., Vincelli, G., Jeffries, C. M., Shaikh, T. R., Pakos, I. S., Ranaivoson, F. M., von Daake, S., Demeler, B., De Jacobo, A., Perkins, G. et al. (2016). Structural characterization of the extracellular domain of CASPR2 and insights into its association with the novel ligand contactin1. *J. Biol. Chem.* **291**, 5788–5802.
- Sanchez-Ponce, D., DeFelipe, J., Garrido, J. J. and Muñoz, A. (2012). Developmental expression of Kv potassium channels at the axon initial segment of cultured hippocampal neurons. *PLoS ONE* **7**, e48557.
- Tanabe, Y., Fujita-Jimbo, E., Momoi, M. Y. and Momoi, T. (2015). CASPR2 forms a complex with GPR37 via MUPP1 but not with GPR37(R558Q), an autism spectrum disorder-related mutation. *J. Neurochem.* **134**, 783–793.
- Traka, M., Goutebroze, L., Denisenko, N., Bessa, M., Niffi, A., Havaki, S., Iwakura, Y., Fukamauchi, F., Watanabe, K., Soliven, B. et al. (2003). Association of TAG-1 with Caspr2 is essential for the molecular organization of juxtaparanodal regions of myelinated fibers. *J. Cell Biol.* **162**, 1161–1172.
- Trimmer, J. S. (2015). Subcellular localization of K⁺ channels in mammalian brain neurons: remarkable precision in the midst of extraordinary complexity. *Neuron* **85**, 238–256.
- Tzamourakas, A., Giasemi, S., Mouratidou, M. and Karagogeos, D. (2007). Structure-function analysis of protein complexes involved in the molecular architecture of juxtaparanodal regions of myelinated fibers. *Biotechnol. J.* **2**, 577–583.
- Van Wart, A., Trimmer, J. S. and Matthews, G. (2007). Polarized distribution of ion channels within microdomains of the axon initial segment. *J. Comp. Neurol.* **500**, 339–352.
- Winckler, B., Forscher, P. and Mellman, I. (1999). A diffusion barrier maintains distribution of membrane proteins in polarized neurons. *Nature* **397**, 698–701.
- Wu, V. M., Yu, M. H., Paik, R., Banerjee, S., Liang, Z., Paul, S. M., Bhat, M. A. and Beitel, G. J. (2007). Drosophila Varicose, a member of a new subgroup of basolateral MAGUKs, is required for septate junctions and tracheal morphogenesis. *Development* **134**, 999–1009.
- Yoshimura, T. and Rasband, M. N. (2014). Axon initial segments: diverse and dynamic neuronal compartments. *Curr. Opin. Neurobiol.* **27**, 96–102.
- Zhou, D., Lambert, S., Malen, P. L., Carpenter, S., Boland, L. M. and Bennett, V. (1998). AnkyrinG is required for clustering of voltage-gated Na channels at axon initial segments and for normal action potential firing. *J. Cell Biol.* **143**, 1295–1304.